LETTER

doi:10.1038/nature12435

Catalytic conversion of nitrogen to ammonia by an iron model complex

John S. Anderson[1], Jonathan Rittle[1] & Jonas C. Peters[1]

The reduction of nitrogen (N_2) to ammonia (NH_3) is a requisite transformation for life[1]. Although it is widely appreciated that the iron-rich cofactors of nitrogenase enzymes facilitate this transformation[2–5], how they do so remains poorly understood. A central element of debate has been the exact site or sites of N_2 coordination and reduction[6,7]. In synthetic inorganic chemistry, an early emphasis was placed on molybdenum[8] because it was thought to be an essential element of nitrogenases[3] and because it had been established that well-defined molybdenum model complexes could mediate the stoichiometric conversion of N_2 to NH_3 (ref. 9). This chemical transformation can be performed in a catalytic fashion by two well-defined molecular systems that feature molybdenum centres[10,11]. However, it is now thought that iron is the only transition metal essential to all nitrogenases[3], and recent biochemical and spectroscopic data have implicated iron instead of molybdenum as the site of N_2 binding in the FeMo-cofactor[12]. Here we describe a tris(phosphine)borane-supported iron complex that catalyses the reduction of N_2 to NH_3 under mild conditions, and in which more than 40 per cent of the proton and reducing equivalents are delivered to N_2. Our results indicate that a single iron site may be capable of stabilizing the various N_xH_y intermediates generated during catalytic NH_3 formation. Geometric tunability at iron imparted by a flexible iron–boron interaction in our model system seems to be important for efficient catalysis[13–15]. We propose that the interstitial carbon atom recently assigned in the nitrogenase cofactor may have a similar role[16,17], perhaps by enabling a single iron site to mediate the enzymatic catalysis through a flexible iron–carbon interaction[18].

Nitrogen is fixed on a vast scale by the industrial Haber–Bosch process using a solid-state Fe catalyst at very high temperatures and pressures, and in nature by nitrogenase enzymes under ambient conditions[1]. These enzymes feature active-site cofactors rich in S and Fe (FeFe-cofactor), and can additionally contain a Mo (FeMo-cofactor; Fig. 1) or V (FeV-cofactor) site[2,3].

The intimate mechanism of biological nitrogen fixation is a topic that has fascinated chemists, biochemists and biologists[4–7]. Synthetic chemists have searched for decades for well-defined complexes that can catalyse N_2 reduction to NH_3[19–22]. Chatt's early work with low-valent Mo complexes provided a mechanistic outline for approaching this problem now commonly called the Chatt, or distal, mechanism, wherein a terminal nitride intermediate is generated on liberation of the first NH_3 equiv. (ref. 9; Fig. 1, bottom). Other mechanisms, including an 'alternating' scenario (Fig. 1, top), have also received attention[6]. So far, even modest catalysis of NH_3 production directly from N_2 by a well-defined model complex is still limited to the original tri(amido)amine Mo systems[10] and the more recently discovered phosphine-pincer Mo system[11]. Earlier work had established the electrochemical feasibility of an NH_3 production cycle with W (ref. 19).

Synthetic efforts to establish whether one or more Fe sites can catalyse N_2 reduction to NH_3 in a well-defined model complex have progressed more slowly. For example, previous Fe–N_2 model complexes have not afforded more than ~10% of NH_3 per Fe equiv. on treatment with proton sources[7,23,24]. Despite important advances[24], which have most recently included reductive N_2 cleavage at Fe (ref. 22) and the catalytic reductive silylation of N_2 facilitated by unknown Fe species derived from Fe precursors such as ferrocene and iron pentacarbonyl[25], the delivery of protons and electrons to N_2 to generate NH_3 catalytically at a synthetic Fe complex has remained an unsolved challenge. Here we show that a recently reported mononuclear Fe complex[13,14], $[(TPB)Fe(N_2)][Na(12\text{-crown-}4)_2]$ (TPB, tris(phosphine)borane; Fig. 2a), can catalyse the reduction of N_2 to NH_3 by protons and electrons in solution at −78 °C under one atmosphere of N_2.

The Fe centre of the '(TPB)Fe' fragment readily binds N_2 as evidenced by the featured five-coordinate complex $[(TPB)Fe(N_2)][Na(12\text{-crown-}4)_2]$ and the previously reported neutral N_2 adduct, $(TPB)Fe(N_2)$ (ref. 14). The same scaffold also accommodates a variety of other nitrogenous ligands relevant to NH_3 generation, including terminally bonded

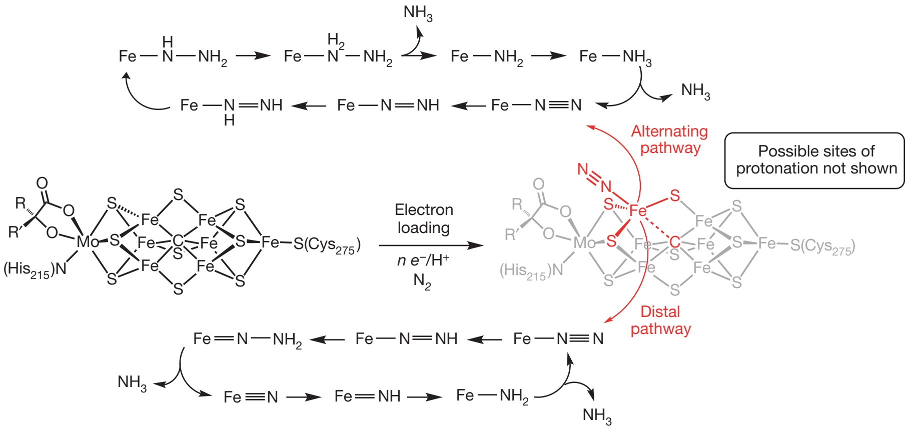

Figure 1 | Chemical line representations of the FeMo-cofactor of nitrogenase. A schematic depiction of postulated N_2 binding and reduction at an Fe site by limiting alternating (top) and distal (bottom) mechanisms. The drawing emphasizes a possible hemilabile role for the interstitial C atom with respect to an Fe–N_2 binding site.

---

[1] Division of Chemistry and Chemical Engineering, California Institute of Technology, Pasadena, California 91125, USA.

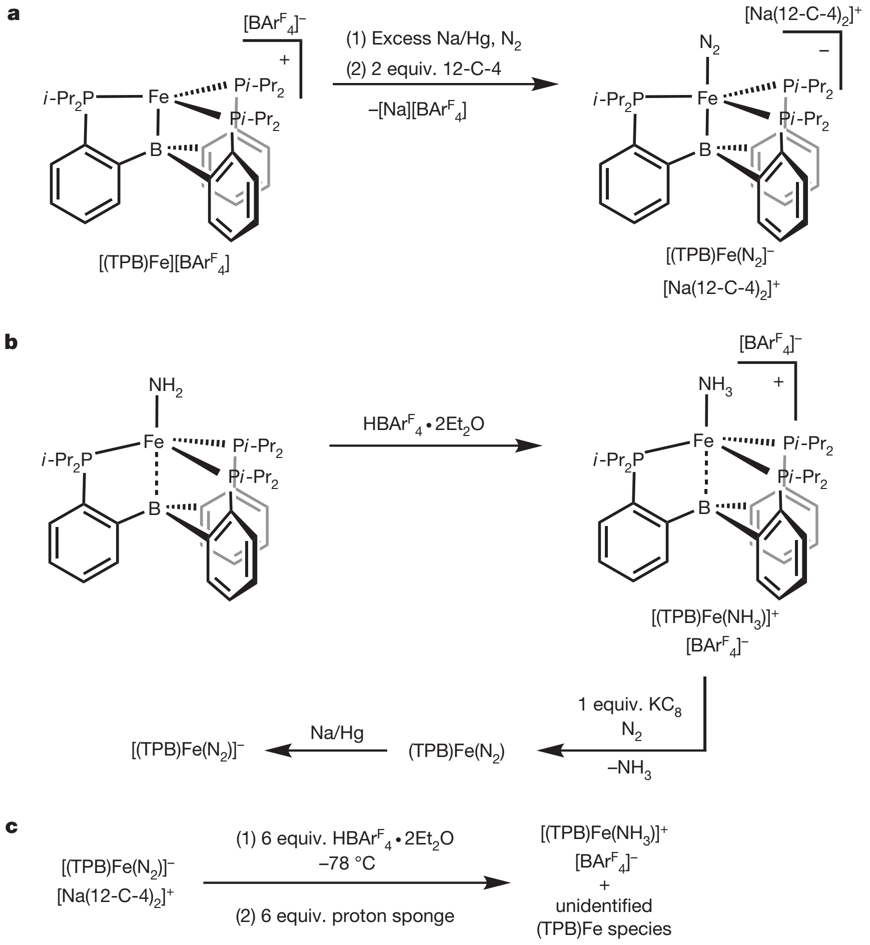

Figure 2 | Stoichiometric (TPB)Fe–N_2 model reactions. **a**, N_2 binding to [(TPB)Fe][$BAr^F{}_4$] under electron loading to generate [(TPB)Fe(N_2)][Na(12-crown-4)$_2$]. **b**, Reductive protonolysis of (TPB)Fe(NH_2) to release NH_3 with concomitant N_2 uptake. **c**, Generation of [(TPB)Fe(NH_3)][$BAr^F{}_4$] and other (TPB)Fe species on addition of acid to [(TPB)Fe(N_2)][Na(12-crown-4)$_2$] at low temperature, followed by warming and then addition of base. 12-C-4, 12-crown-4.

NH_2, NH_3 and N_2H_4 ligands[15]. Both the substrate-free complex, [(TPB)Fe][$BAr^F{}_4$] (where [$BAr^F{}_4$]$^-$ represents the weakly coordinating anion [B(3,5-(CF_3)$_2$-C_6H_3)$_4$]$^-$; ref. 15), and (TPB)Fe(N_2) may be reduced to [(TPB)Fe(N_2)][Na(12-crown-4)$_2$] by Na/Hg reduction under 1 atm N_2 followed by the addition of 2 equiv. of 12-crown-4 to encapsulate the sodium cation (Fig. 2a). Model reactions with silyl electrophiles have also shown that the Nβ of the coordinated N_2 ligand can be mono- or difunctionalized with concomitant increase in the Fe–B distance[13]. Furthermore, starting from (TPB)Fe(NH_2), a reductive protonation sequence has been established (Fig. 2b) that liberates NH_3 and affords (TPB)Fe(N_2) (ref. 15). This reaction sequence demonstrates the synthetic viability of reductive release of NH_3 from an Fe–NH_2 intermediate with simultaneous uptake of N_2. In sum, the rich reaction chemistry of the (TPB)Fe scaffold with nitrogenous ligands motivated us to examine more closely the possibility that it might catalyse N_2 fixation.

The addition of excess acid to [(TPB)Fe(N_2)][Na(12-crown-4)$_2$] at $-78\,^{\circ}$C was investigated (Fig. 2c). When [(TPB)Fe(N_2)][Na(12-crown-4)$_2$] was dissolved in tetrahydrofuran (THF), cooled to $-78\,^{\circ}$C and exposed to 6 equiv. of H^+ in the form of $HBAr^F{}_4 \cdot 2Et_2O$, a previously unobserved yellow solution resulted that, on warming followed by addition of proton sponge (1,8-bis(dimethylamino)naphthalene), was shown by ^{1}H NMR analysis to contain the previously characterized complex[15] [(TPB)Fe(NH_3)][$BAr^F{}_4$] (~30–35% of the total Fe), along with resonances consistent with [(TPB)Fe][$BAr^F{}_4$] (~40–45% of the total Fe) and two other minor and as yet unidentified paramagnetic (TPB)Fe-species (Supplementary Information). An independent electron paramagnetic resonance (EPR) study of this low-temperature protonation reaction in 2-methyltetrahydrofuran revealed a new rhombic $S = 1/2$ signal (Supplementary Information) that we speculate may be (TPB)Fe(=N–NH_2)$^+$ or an alternative structural isomer such as (TPB)Fe(NH=NH)$^+$. Spin quantification of this species showed it to represent >85% of the Fe species in solution, and its rhombic EPR spectrum is highly similar to the rhombic EPR signature that is obtained on oxidation of (TPB)Fe=N(*p*-tolyl) to generate (TPB)Fe=N(*p*-tolyl)$^+$ (Supplementary Information). Subsequent low-temperature reduction of a similarly prepared mixture regenerates [(TPB)Fe(N_2)][Na(12-crown-4)$_2$], as determined by infrared spectroscopy, suggesting the possibility of cycling protonation and reduction with this Fe system.

To explore the possibility of N_2 reduction catalysis using this (TPB)Fe system, we tested several reductants (for example Na[naphthalenide], Mg(THF)$_3$(anthracene), Na/Hg and KC_8) and acids (for example HCl, trifluoromethanesulphonic acid and $HBAr^F{}_4 \cdot 2Et_2O$) in a variety of solvents and solvent mixtures (for example THF, dimethoxyethane, diethyl ether and toluene). When carried out at $-78\,^{\circ}$C numerous reaction conditions showed unusually high yields of NH_3 relative to the number of Fe equivalents in the reaction vessel, and the combination of KC_8, $HBAr^F{}_4 \cdot 2Et_2O$ and Et_2O solvent enabled the catalytic generation of NH_3.

In a representative catalytic run, red [(TPB)Fe(N_2)][Na(12-crown-4)$_2$] was suspended in diethyl ether in a reaction vessel at $-78\,^{\circ}$C, followed by the sequential addition of excess acid and then excess reductant. Ammonia analysis followed the indophenol protocol (Methods and Supplementary Information) and the independent identification of ammonium salts by ^{1}H NMR spectroscopy in dimethylsulphoxide

(DMSO) by comparison with an authentic sample of $[NH_4][Cl]$ (Fig. 3a). An experiment performed using the $[(TPB)Fe(^{14}N_2)][Na(12\text{-crown-}4)_2]$ catalyst under an $^{15}N_2$ atmosphere, followed by ^1H NMR analysis (Fig. 3a) of the volatile reaction products, confirmed the production of $[^{15}NH_4][Cl]$, as expected, with only trace $[^{14}NH_4][Cl]$. This overall procedure has been repeated many times, and Table 1 includes data averaged from 16 independent runs (entry 1) in which yields were, on average, 7.0 equiv. NH_3 per Fe equiv. Using 7.0 equiv. NH_3 as the product stoichiometry, 44% of the added protons are reliably delivered to N_2 to produce NH_3. Our individual runs reached a maximum of 8.5 equiv. NH_3 per Fe equiv. under these standard conditions. $[(TPB)Fe][BAr^F_4]$ is also an effective catalyst and afforded 6.2 ± 0.7 equiv. NH_3 per added Fe equiv. (Table 1, entry 2). For comparison, the Mo systems of refs 10, 11 have afforded between 7 and 12 equiv. NH_3 per Mo equiv. The current Fe system seems to be active at an unusually low temperature (-78 °C) but benefits from a strong reductant (KC_8). We do not yet know whether conditions can be found that will tolerate a milder reductant, for example by circumventing the need to generate the $(TPB)Fe(N_2)^-$ anion during catalysis.

Table 1 lists several sets of conditions (entries 10–15) other than the standard conditions described above that were studied. Several of these alternative conditions showed NH_3 generation, although not in catalytic or even in high yields. N_2H_4 was not detected as an additional product when using the standard catalytic protocol for NH_3 generation with $[(TPB)Fe(N_2)][Na(12\text{-crown-}4)_2]$ (Supplementary Information). If 2 equiv. N_2H_4 (per Fe) were added to $[(TPB)Fe(N_2)][Na(12\text{-crown-}4)_2]$ in diethyl ether and the mixture was then subjected to the standard catalytic conditions and work-up, only trace N_2H_4 remained (Supplementary Information). This result suggests that if N_2H_4 is generated as an intermediate during catalysis, it would not likely be detectable on work-up and analysis. It is worth noting that $HBAr^F_4\cdot 2Et_2O$ and KC_8 react in the absence of an Fe precursor, under the standard catalytic conditions at -78 °C, to generate H_2 but not NH_3 (>75% yield of H_2 after 40 min). That H_2 generation is kinetically feasible without the addition of an Fe precursor, and yet NH_3 can nonetheless be generated on the addition of $[(TPB)Fe(N_2)][Na(12\text{-crown-}4)_2]$ or $[(TPB)Fe][BAr^F_4]$, underscores the facility with which this Fe system mediates overall hydrogen-atom delivery to N_2.

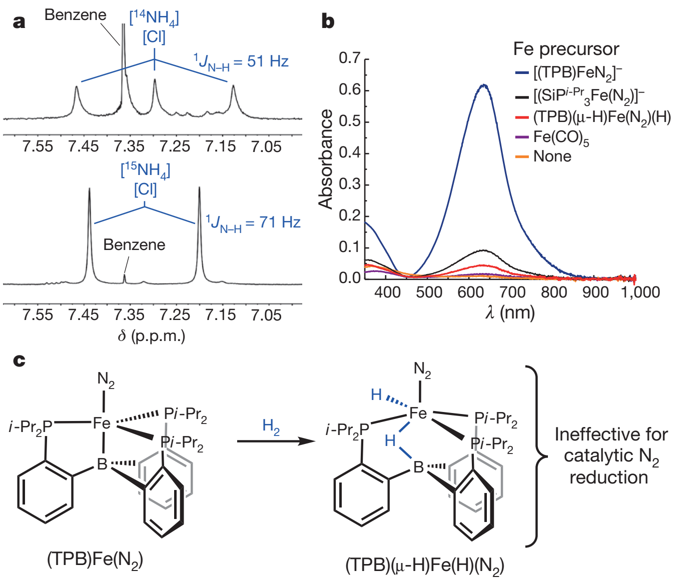

Figure 3 | Spectral data for ammonia analysis, and catalyst poisoning. **a**, ^1H NMR spectrum (300 MHz) of $[^{14}NH_4][Cl]$ in DMSO-d_6 produced from a catalytic run under $^{14}N_2$ (top) and of $[^{15}NH_4][Cl]$ in DMSO-d_6 produced from an independent catalytic run under 1 atm $^{15}N_2$. δ, chemical shift. **b**, Representative optical data for NH_3 product analysis using the indophenol method from catalytic runs using the standard conditions with the precursors indicated. **c**, H_2 binds to $(TPB)Fe(N_2)$ to generate $(TPB)(\mu\text{-}H)Fe(N_2)(H)$, which itself is ineffective for the catalytic generation of NH_3 from N_2 under the standard conditions.

Table 1 | Ammonia generation from N_2 mediated by Fe precursors

$$\begin{array}{c}\text{Excess }HBAr^F_4\cdot 2Et_2O\\ +\\ \text{Excess }KC_8\end{array} \quad N_2 \xrightarrow[\begin{array}{c}Et_2O\\ -78\ °C\end{array}]{\begin{array}{c}\text{Fe}\\ \text{catalyst}\end{array}} NH_3$$

Using standard catalytic conditions as described in the text

Entry	Fe precursor	NH_3 equiv./Fe†
1	$[(TPB)Fe(N_2)][Na(12\text{-crown-}4)_2]$	7.0 ± 1‡
2	$[(TPB)Fe][BAr^F_4]$	6.2
3	$[(SiP^{i\text{-}Pr}_3)Fe(N_2)][Na(12\text{-crown-}4)_2]$	0.7
4	$(TPB)(\mu\text{-}H)Fe(N_2)(H)$	0.5
5	$FeCl_2\cdot 1.5THF$	<0.1
6	$FeCl_3$	<0.1
7	Cp_2Fe	<0.2
8	$Fe(CO)_5$	<0.1
9	None	<0.1

Variations on standard conditions using $[(TPB)FeN_2][Na(12\text{-crown-}4)_2]$

Entry	Variation	NH_3 equiv./Fe†
10	HOTf as acid	0.4
11	$[\text{Lutidinium}][BAr^F_4]$ as acid	<0.1
12	HCl as acid	<0.1
13	Cp^*_2Co as reductant	0.6
14	Cp^*_2Cr as reductant	<0.2
15	K metal as reductant	0.4

† NH_3 was collected by vacuum transfer of the reaction volatiles into HCl in diethyl ether. A dimethoxyethane solution of [Na][O*t*-Bu] (20 equiv. relative to Fe) was added to the reaction vessel residue, followed by an additional vacuum transfer, to ensure complete liberation of all NH_3. The $[NH_4][Cl]$ precipitate formed in the acidic Et_2O collection vessel was reconstituted in deionized H_2O, from which an aliquot was taken for indophenol quantification. Analysis of the $[NH_4][Cl]$ formed by ^1H NMR spectroscopy in DMSO, compared with an authentic sample, provided independent confirmation of NH_3 generation. Data for individual experimental runs, and additional runs using potential precatalysts that are not presented in this table, are provided in Supplementary Information. Unless noted otherwise, all yields are reported as an average of 4 runs.

‡ Average of 16 runs.

HOTf, trifluoromethanesulphonic acid; *i*-Pr, isopropyl; lutidinium, 2,6-dimethylpyridinium; *t*-Bu, *tert*-butyl.

To explore further whether a (TPB)Fe-containing precursor is needed to facilitate the overall catalysis, beyond the stoichiometric model reactions summarized above, we canvassed several Fe complexes under analogous conditions. Of most interest is the complex $[(SiP^{i\text{-}Pr}_3)Fe(N_2)][Na(12\text{-crown-}4)_2]$, which is isostructural to $[(TPB)Fe(N_2)][Na(12\text{-crown-}4)_2]$ but in which the B atom of TPB is replaced by a Si atom[26]. A central difference between (TPB)Fe and $(SiP^{i\text{-}Pr}_3)$Fe complexes is the far greater flexibility of the Fe–B bond by comparison with the Fe–Si bond that is positioned *trans* to the apical ligand[13–15,26]. Although some NH_3 generation was observed for $[(SiP^{i\text{-}Pr}_3)Fe(N_2)][Na(12\text{-crown-}4)_2]$ when subjected to the standard catalytic reaction conditions described above, substoichiometric yields of NH_3 relative to Fe were obtained (0.7 ± 0.5 equiv. NH_3 per Fe equiv.; Table 1, entry 3). We also conducted additional control experiments under the standard catalytic conditions with $FeCl_2\cdot 1.5THF$, $FeCl_3$, Cp_2Fe (ref. 25) and $Fe(CO)_5$ (ref. 25) (entries 5–8) and found that only trace amounts of NH_3 (<0.2 equiv. in all cases on average; four runs) were produced by these Fe precursors[27] (Supplementary Information). The known phosphine-supported Fe(0)–N_2 complex $Fe(depe)_2(N_2)$ (ref. 28) was also subjected to the standard conditions and afforded sub-stoichiometric yields of NH_3 per Fe equiv. (Supplementary Information).

In separate work, the addition of H_2 to $(TPB)Fe(N_2)$ was shown to generate $(TPB)(\mu\text{-}H)Fe(N_2)(H)$ as a stable product[29] (Fig. 3c). We hence suspected that catalyst poisoning might occur in part through the formation of $(TPB)(\mu\text{-}H)Fe(N_2)(H)$ under the catalytic reaction conditions. In accord with this idea, when $[(TPB)Fe(N_2)][Na(12\text{-crown-}4)_2]$ was exposed to 10 equiv. $HBAr^F_4\cdot 2Et_2O$ and 12 equiv. KC_8 at low temperature, infrared and ^{31}P NMR analysis of the resulting mixture showed the presence of $(TPB)(\mu\text{-}H)Fe(N_2)(H)$ through its signature spectroscopic features[29] (30% of total Fe by ^{31}P NMR integration;

Supplementary Information). (TPB)(μ-H)Fe(N_2)(H) is stable for short periods to both $HBAr^F{}_4 \cdot 2Et_2O$ and also KC_8 in Et_2O at room temperature, and when subjected to the standard catalytic conditions for NH_3 production liberates only 0.5 ± 0.1 equiv. NH_3 per Fe equiv. (Table 1, entry 4, and Fig. 3b).

The general absence of a functional, catalytic Fe model system over the past few decades has often led to an emphasis on Mo (ref. 30) as a plausible site of N_2 uptake and reduction at the most widely studied FeMo-cofactor. Although this may yet prove to be true, recent spectroscopic and biochemical evidence has sharpened the focus on an Fe centre as the N_2-binding site[12]. The results reported here establish that it is possible to catalyse the conversion of N_2 to NH_3 by protons and electrons using a well-defined mononuclear Fe–N_2 complex, and suggests the possibility that a single Fe-binding site of the cofactor could in principle mediate N_2 reduction catalysis[18]. To achieve this catalytic behaviour, geometric flexibility at the Fe–N_2 binding site would be beneficial as it would stabilize N_xH_y intermediates with different electronic structure requirements. Such geometric and redox flexibility, under the local three-fold symmetry presented by an Fe centre, its three neighbouring sulphides and the interstitial light atom of the FeMo-cofactor[16,17], may at least in part be achieved by attributing a hemilabile role to the interstitial C atom (Fig. 1). Such a role could serve to expose an initial Fe–N_2 binding site by Fe–C elongation. Subsequent modulation of the Fe–C interaction and, hence, the local Fe geometry as a function of the N_2 reduction state would enable the Fe centre to stabilize the various N_xH_y intermediates along a pathway to NH_3. Although it is inherently speculative, this hypothesis is rooted in the functional (TPB)Fe catalysis discussed here, along with the types of (TPB)Fe complex and stoichiometric transformation described previously for this scaffold[13–15].

Many mechanistic questions arise from the present Fe catalyst system. Although all of the model complexes relevant to the (TPB)Fe–N_xH_y system are mononuclear, we cannot exclude the possibility of bimolecular reaction intermediates. More generally, we do not know whether the N_2 reduction catalysis proceeds along a distal pathway via a terminal nitride intermediate, such as (TPB)Fe(N) or $(TPB)Fe(N)^+$, via intermediates along an alternating pathway, such as (TPB)Fe–NH–NH_2 or (TPB)Fe–NH_2–$NH_2{}^+$, or via some hybrid pathway. The tentatively assigned (TPB)Fe=N–$NH_2{}^+$ species that can be observed by EPR spectroscopy provides us with a useful starting point for such studies. In light of the identification of C as the interstitial light atom of the cofactor, it is also of interest to develop and compare synthetic model systems that feature a C atom in the ligand backbone instead of a B atom.

METHODS SUMMARY

General considerations. All complexes and reagents were prepared according to literature procedures referenced in the Supplemental Information unless otherwise noted. Manipulations were carried out under an N_2 atmosphere utilizing standard dry glove-box or Schlenk-line techniques. All solvents used were deoxygenated and dried by N_2 sparging followed by passage through an activated alumina column.

Spectroscopy. NMR measurements were made using Varian 300-MHz spectrometers. Deuterated solvents for these measurements were obtained from Cambridge Isotope Laboratories and were dried and degassed before use. All ^1H NMR spectra were referenced to residual solvent peaks. EPR X-band spectra were obtained on a Bruker EMX spectrometer with the aid of the Bruker WIN-EPR software suite, version 3.0. The EPR spectrometer was equipped with a rectangular cavity that operated in the TE_{102} mode. Temperature control was achieved with a liquid-N_2-filled quartz Dewar flask in which the sample was submerged during data collection. Ultraviolet–visible spectra were acquired on a Cary 50 spectrometer from 1,100 to 200 nm in the fast-scan mode. Infrared spectra were obtained using KBr pellets on a Bio-Rad Excalibur FTS 3000 spectrometer using Varian RESOLUTIONS PRO software set at a resolution of 4 cm^{-1}.

Catalysis and ammonia collection and quantification. The standard catalysis protocol involved the addition of first acid and then reductant to a suspension of the precatalyst in diethyl ether at $-78\,^{\circ}C$ in a closed vessel under 1 atm N_2. Ammonia produced during each catalytic run was collected by vacuum transfer of the reaction volatiles onto anhydrous HCl in diethyl ether. The resulting slurry was dried and extracted into water and aliquots were then tested for the presence of ammonia by the indophenol method.

Full Methods and any associated references are available in the online version of the paper.

Received 8 February; accepted 4 July 2013.

1. Smil, V. *Enriching the Earth* (MIT Press, 2001).
2. Burgess, B. K. & Lowe, D. J. Mechanism of molybdenum nitrogenase. *Chem. Rev.* **96,** 2983–3012 (1996).
3. Eady, R. R. Structure-function relationships of alternative nitrogenases. *Chem. Rev.* **96,** 3013–3030 (1996).
4. Howard, J. B. & Rees, D. C. How many metals does it take to fix N_2? A mechanistic overview of biological nitrogen fixation. *Proc. Natl Acad. Sci. USA* **103,** 17088–17093 (2006).
5. Schwarz, G., Mendel, R. R. & Ribbe, M. W. Molybdenum cofactors, enzymes and pathways. *Nature* **460,** 839–847 (2009).
6. Seefeldt, L., Hoffman, B. M. & Dean, D. R. Mechanism of Mo-dependent nitrogenase. *Annu. Rev. Biochem.* **78,** 701–722 (2009).
7. Peters, J. C. & Mehn, M. P. in *Activation of Small Molecules: Organometallic and Bioinorganic Perspectives* (ed. Tolman, W. B.) 81–119 (Wiley-VCH, 2006).
8. Shilov, A. E. *et al.* New nitrogenase model for reduction of molecular nitrogen in protonic media. *Nature* **231,** 460–461 (1971).
9. Chatt, J., Dilworth, J. R. & Richards, R. L. Recent advances in chemistry of nitrogen-fixation. *Chem. Rev.* **78,** 589–625 (1978).
10. Yandulov, D. V. & Schrock, R. R. Catalytic reduction of dinitrogen to ammonia at a single molybdenum center. *Science* **301,** 76–78 (2003).
11. Arashiba, A., Miyake, Y. & Nishibayashi, Y. A molybdenum complex bearing PNP-type pincer ligands leads to the catalytic reduction of dinitrogen into ammonia. *Nature Chem.* **3,** 120–125 (2011).
12. Hoffman, B. M., Dean, D. R. & Seefeldt, L. C. Climbing nitrogenase: toward a mechanism of enzymatic nitrogen fixation. *Acc. Chem. Res.* **42,** 609–619 (2009).
13. Moret, M.-E. & Peters, J. C. N_2 functionalization at iron metallaboratranes. *J. Am. Chem. Soc.* **133,** 18118–18121 (2011).
14. Moret, M.-E. & Peters, J. C. Terminal iron dinitrogen and iron imide complexes supported by a tris(phosphino)borane ligand. *Angew. Chem. Int. Ed.* **50,** 2063–2067 (2011).
15. Anderson, J. A., Moret, M.-E. & Peters, J. C. Conversion of Fe–NH_2 to Fe–N_2 with release of NH_3. *J. Am. Chem. Soc.* **135,** 534–537 (2013).
16. Lancaster, K. M. *et al.* X-ray emission spectroscopy evidences a central carbon in the nitrogenase iron-molybdenum cofactor. *Science* **334,** 974–977 (2011).
17. Spatzal, T. M. *et al.* Evidence for interstitial carbon in nitrogenase FeMo cofactor. *Science* **334,** 940 (2011).
18. Hendrich, M. P. *et al.* On the feasibility of N_2 fixation via a single-site Fe^I/Fe^{IV} cycle: spectroscopic studies of $Fe^I(N_2)Fe^I$, $Fe^{IV}{\equiv}N$, and related species. *Proc. Natl Acad. Sci. USA* **103,** 17107–17112 (2006).
19. Pickett, C. J. & Talarmin, J. Electrosynthesis of ammonia. *Nature* **317,** 652–653 (1985).
20. Fryzuk, M. D., Love, J. B., Rettig, S. J. & Young, V. G. Transformation of coordinated dinitrogen by reaction with dihydrogen and primary silanes. *Science* **275,** 1445–1447 (1997).
21. Pool, J. A., Lobkovsky, E. & Chirik, P. J. Hydrogenation and cleavage of dinitrogen to ammonia with a zirconium complex. *Nature* **427,** 527–530 (2004).
22. Rodriguez, M. M., Bill, E., Brennessel, W. W. & Holland, P. L. N_2 reduction and hydrogenation to ammonia by a molecular iron-potassium complex. *Science* **334,** 780–783 (2011).
23. Hills, A. *et al.* Bis[1,2-bis(dimethylphosphino)ethane]dihydrogenhydridoiron(II) tetraphenylborate as a model for the function of nitrogenases. *J. Chem. Soc. Dalton Trans.* **25,** 3041–3049 (1993).
24. Crossland, J. L. & Tyler, D. R. Iron-dinitrogen coordination chemistry: dinitrogen activation and reactivity. *Coord. Chem. Rev.* **255,** 949–974 (2011).
25. Yuki, M., Tanaka, H., Miyake, Y., Yoshizawa, K. & Nishibayashi, Y. Iron-catalysed transformation of molecular dinitrogen into silylamine under ambient conditions. *Nature Commun.* **3,** 1254 (2012).
26. Lee, Y. H., Mankad, N. P. & Peters, J. C. Triggering N_2 uptake via redox-induced expulsion of coordinated NH_3 and N_2 silylation at trigonal bipyramidal iron. *Nature Chem.* **2,** 558–565 (2010).
27. Bell, L. G. & Brintzinger, H. H. Stoichiometric reduction of molecular nitrogen by iron complexes. *J. Am. Chem. Soc.* **92,** 4464–4465 (1970).
28. Hall, D. A. & Leigh, G. J. Reduction of dinitrogen bound at an iron(0) centre. *J. Chem. Soc. Dalton Trans.* 3539–3541 (1996).
29. Fong, H., Moret, M.-E., Lee, Y. H. & Peters, J. C. Heterolytic H_2 cleavage and catalytic hydrogenation by an iron metallaboratrane. *Organometallics* **32,** 3053–3062 (2013).
30. Schrock, R. R. Nitrogen reduction: molybdenum does it again. *Nature Chem.* **3,** 95–96 (2011).

Supplementary Information is available in the online version of the paper.

Acknowledgements This work was supported by the NIH (GM 070757) and the Gordon and Betty Moore Foundation. A. Takaoka is thanked for developing the calibration curves used for ammonia and hydrazine quantification. D. Rees and D. Newman are acknowledged for many discussions.

Author Contributions J.S.A., J.R. and J.C.P. designed the study. J.S.A. and J.R. conducted the experiments. J.S.A., J.R. and J.C.P. interpreted the data. J.S.A., J.R. and J.C.P. wrote the manuscript.

Author Information Reprints and permissions information is available at www.nature.com/reprints. The authors declare no competing financial interests. Readers are welcome to comment on the online version of the paper. Correspondence and requests for materials should be addressed to J.C.P. (jpeters@caltech.edu).

METHODS

General considerations. We prepared [(TPB)Fe(N$_2$)][Na(12-crown-4)$_2$] (ref. 14), [(TPB)Fe][BAr$^{\mathrm{F}}_4$] (ref. 15), (TPB)(μ-H)Fe(H)(N$_2$) (ref. 29), [lutidinium][BAr$^{\mathrm{F}}_4$] (ref. 31), HBAr$^{\mathrm{F}}_4$·2Et$_2$O (ref. 32), [(SiP$^{i\text{-Pr}}_3$)Fe(N$_2$)][Na(12-crown-4)$_2$] (ref. 26), FeCl$_2$·(THF)$_{1.5}$ (ref. 33), KC$_8$ (ref. 34), [(TPB)Fe(NH$_3$)][BAr$^{\mathrm{F}}_4$] (ref. 15), [(TPB)Fe(N$_2$H$_4$)][BAr$^{\mathrm{F}}_4$] (ref. 15) and Fe(depe)$_2$N$_2$ (ref. 28) were prepared according to literature procedures. Labelled ^{15}N$_2$ (98% purity) was obtained from Cambridge Isotope Laboratories. Solvents used for catalytic runs were additionally stirred for more than 2 h over Na/K alloy and then filtered before use, and subjected to standard sparging (Ar gas) and passage through an activated alumina column.

Ammonia quantification. A Schlenk tube was charged with HCl (3 ml of a 2.0 M solution in Et$_2$O, 6 mmol). Reaction mixtures were vacuum-transferred into this collection flask. Residual solid in the reaction vessel was treated with a solution of [Na][O-*t*-Bu] (40 mg, 0.4 mmol) in 1,2-dimethoxyethane (1 ml) and sealed. The resulting suspension was stirred for 10 min before all volatiles were again vacuum-transferred into the collection flask. After completion of the vacuum transfer, the flask was sealed and warmed to room temperature. Solvent was removed *in vacuo* and the remaining residue was dissolved in H$_2$O (1 ml). An aliquot of this solution (20 or 40 μl) was then analysed for the presence of NH$_3$ (trapped as [NH$_4$][Cl]) by the indophenol method[35]. Quantification was performed with ultraviolet–visible spectroscopy by analysing absorbance at 635 nm. The tables in Supplementary Information show the raw data for the runs. Runs with small absorbance levels ($<$0.02 absorbance units) suffer from a large degree of error due to a small signal-to-noise ratio. Catalytic runs that used a 40 μl aliquot are denoted with an asterisk, accounting for larger relative absorbances.

Standard catalytic protocol. We suspended [(TPB)Fe(N$_2$)][Na(12-crown-4)$_2$] (2 mg, 0.002 mmol) in Et$_2$O (0.5 ml) in a 20-ml scintillation vial equipped with a stir bar. This suspension was vigorously stirred and cooled to −78 °C in a cold well inside the glove box. A similarly cooled solution of HBAr$^{\mathrm{F}}_4$·2Et$_2$O (93 mg, 0.092 mmol) in Et$_2$O (1.5 ml) was added to the suspension in one portion with rapid stirring. Any remaining acid was dissolved in cold Et$_2$O (0.25 ml) and added subsequently. The reaction mixture turned light yellow-orange and became homogeneous on addition of acid, and the resulting solution was stirred for 5 min before being transferred into a pre-cooled Schlenk tube equipped with a stir bar. The original reaction vial was washed with cold Et$_2$O (0.25 ml) and was subsequently transferred to the Schlenk tube. Solid KC$_8$ (15 mg, 0.100 mmol) was suspended in cold Et$_2$O (0.75 ml) and added drop by drop to the rapidly stirred solution in the Schlenk tube, which was then tightly sealed. The reaction was stirred for 40 min at −78 °C before being warmed to room temperature and stirred for a further 15 min.

Detailed experimental procedures and data for all experiments can be found in Supplemental Information.

31. Yandulov, D. V. & Schrock, R. R. Reduction of dinitrogen to ammonia at a well-protected reaction site in a molybdenum triamidoamine complex. *J. Am. Chem. Soc.* **124,** 6252–6253 (2002).
32. Brookhart, M., Grant, B. & Volpe, A. F., Jr. [(3,5-(CF$_3$)$_2$C$_6$H$_3$)$_4$B]$^-$[H(OEt$_2$)$_2$]$^+$: a convenient reagent for generation and stabilization of cationic, highly electrophilic organometallic complexes. *Organometallics* **11,** 3920–3922 (1992).
33. Kern, R. J. Tetrahydrofuran complexes of transition metal chlorides. *J. Inorg. Nucl. Chem.* **24,** 1105–1109 (1962).
34. Weitz, I. S. & Rabinovitz, M. The application of C$_8$K for organic synthesis: reduction of substituted naphthalenes. *J. Chem. Soc. Perkin Trans.* **1,** 117–120 (1993).
35. Weatherburn, M. W. Phenol-hypochlorite reaction for determination of ammonia. *Anal. Chem.* **39,** 971–974 (1967).